

# BEAM DYNAMICS DESIGN OF THE 211 MEV APT NORMAL CONDUCTING LINAC \*

L. M. Young, J. H. Billen, H. Takeda, R. L. Wood

Los Alamos National Laboratory, MS H817, Los Alamos, NM 87545, USA

## Abstract

This paper describes the normal conducting linac design that is part of the Accelerator for Production of Tritium (APT) project [1]. The new version of PARMILA [2] designed this linac. This linac accepts the beam from the 6.7-MeV radio-frequency quadrupole (RFQ) [3,4] without a separate matching section. At about 10 MeV, it has a smooth transition in the length of period from  $8\beta\lambda$  to  $9\beta\lambda$  in quadrupole focusing lattice. This adjustment of the period was needed to provide sufficient space for the quadrupole focusing magnets and beam diagnostic equipment. The linac consists of the coupled-cavity drift-tube linac (CCDTL) [5] up to 97 MeV and coupled-cavity linac (CCL) above 97 MeV.

## 1 INTRODUCTION

The first 211 MeV of the APT linac consists of the 700-MHz CCDTL and CCL. The CCDTL accepts the beam from the 350-MHz, 6.7-MeV RFQ without a separate matching section. The CCDTL accelerates the 100-mA beam to 97 MeV. The CCL accelerates the beam to 211 MeV. The CCDTL uses a transverse focusing period of  $8\beta\lambda$  from 6.7 MeV to about 9.5 MeV. At this point the transverse focusing period is smoothly increased to  $9\beta\lambda$  to make more room for the quadrupole focusing magnets. The  $8\beta\lambda$  section of the CCDTL uses one accelerating cavity with 1 drift tube between each quadrupole magnet leaving plenty of space for the quadrupole. After the transition to  $9\beta\lambda$  the CCDTL has one accelerating cavity with 2 drift tubes between each quadrupole. The rest of the CCDTL and CCL accelerator use the  $9\beta\lambda$  focusing period. Figure 1 shows the particle coordinates versus cell number from a PARMILA simulation through the 211-MeV linac and the first 6 “Cryomodules” of the Superconducting linac. A “Cryomodule” is a cryostat with two or more accelerating cavities. Each accelerating gap and each quadrupole increments the cell number in this figure.

## 2 RFQ TO CCDTL MATCHING

We used no separate matching section to match the beam from the RFQ to the CCDTL. By adjusting the length of the fringe-field cell at the output of the RFQ, we matched the beam into the CCDTL quadrupole focusing channel. In addition, we adjusted the transverse focusing strength per cm of the RFQ to equal that of the CCDTL so

that the match would be current independent. The longitudinal matching was a little more difficult because the longitudinal focusing goes to zero at the end of the final accelerating cell in the RFQ. Also, the beam drifts to the first cavity of the CCDTL before it sees any longitudinal focusing. Another complication is that the RFQ operates at 350 MHz and the CCDTL at 700 MHz. This problem was solved by setting the synchronous phase of the first accelerating cavity at  $-90^\circ$  and increasing the RF fields in this cavity by a factor of 1.65. The second accelerating cavity was operated at  $-30^\circ$  synchronous

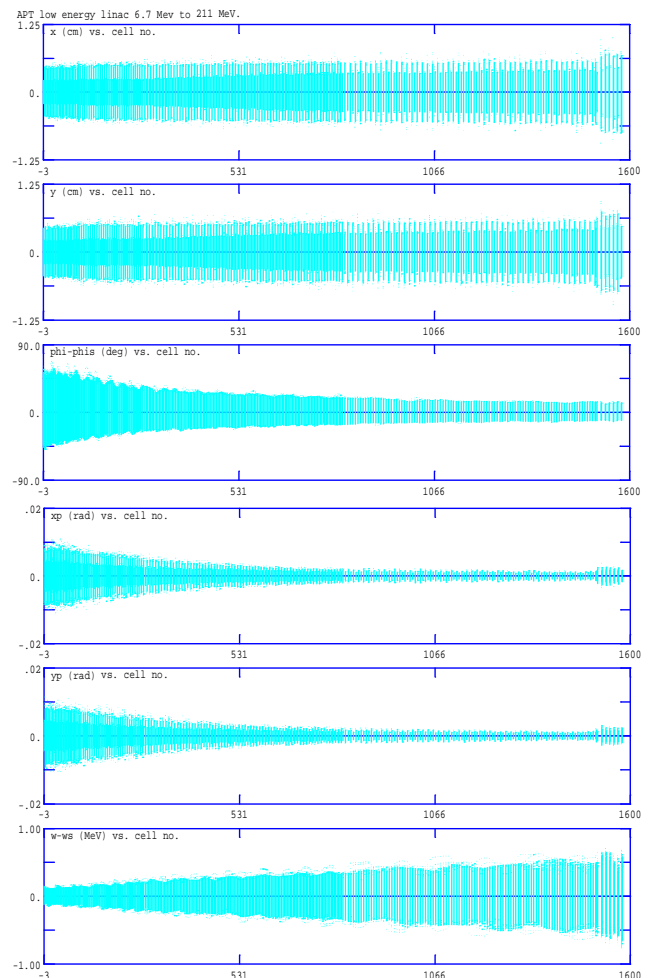


Figure 1. Beam size versus cell number of the 211-MeV APT Linac. Plotted versus cell number respectively from the top down are particle coordinates  $x$ ,  $y$ ,  $\phi$ ,  $x_p$ ,  $y_p$ , and energy. The phase “ $\phi$ ” and the energy are plotted with respect to the phase and energy of the synchronous particle. Divergence coordinates are  $x_p = dx/dz$  and  $y_p = dy/dz$ . This data comes from a PARMILA simulation with 95405 particles.

\*Work supported by the US Department of Energy.

phase and normal RF fields. The third and subsequent accelerating cavities operate at  $-60^\circ$  synchronous phase to provide a large enough longitudinal acceptance to capture the beam bunches from the 350-MHz RFQ. We chose the RF amplitude at the beginning of the CCDTL to provide nearly the same longitudinal focusing strength per cm as provided by the RFQ near its exit. Figure 2 shows the longitudinal and transverse zero-current phase advance divided by the transverse-focusing-period length plotted versus energy from 1 MeV (in the RFQ) to 245 MeV (in the first part of the superconducting accelerator). The small discontinuities in the focusing strength in this figure at 6.7 MeV, show the match in the focusing between the RFQ and the CCDTL.

### 3 CCDTL

The RF amplitude slowly increases and the synchronous phase approaches  $-30^\circ$  as the energy increases. At 10 MeV, after the transition to the  $9\beta\lambda$  focusing period, the real-estate accelerating field is too high for the 1-drift-tube CCDTL. The term real-estate refers to an average over a transverse focusing period. The CCDTL uses 2 drift tubes in each cavity from 10 MeV to 21.6 MeV. At 21.6 MeV the synchronous phase has progressed to  $-40^\circ$  and the accelerating field to 1.863 MeV/m. The accelerating structure only occupies  $5/9^{\text{th}}$  of the real estate. Therefore the real-estate accelerating field is 1.035 MeV/m.

The CCDTL uses 2 cavities with 1 drift tube in each between each quadrupole magnet from 21.6 MeV to 96.7 MeV. The synchronous phase reaches its final value of  $-30^\circ$  at 92 MeV. At that point the effective real-estate accelerating field,  $E_0T$ , is 1.12 MeV/m. We made the changes in the accelerating field and synchronous phase to keep the ratio of the longitudinal and transverse phase advance per cm nearly constant below 25 MeV. Below 25 MeV the transverse phase advance was kept constant at  $\sim 78^\circ$  per period.

The effect of changing the period from  $8\beta\lambda$  to  $9\beta\lambda$  can be seen between 9.5 and 10 MeV in Figure 2. At energies above 25 MeV, we slowly decreased the quadrupole focusing strength as the energy increased. We reduced the quadrupole focusing strength at higher energies for two reasons. First, by keeping the ratio of the longitudinal focusing strength to the transverse focusing strength constant the bunch shape remained nearly constant. Also, as shown in Figure 3, the longitudinal tune depression did not fall to extremely low values as it would have without reducing the transverse focusing strength. Second, we had to reduce the transverse focusing strength at the end of the normal conducting linac to equal that available at the beginning of the superconducting linac.

### 4 CCL

The linac uses the CCL structure from 96.7 MeV to 211 MeV. The first segment in each module uses 6

accelerating cavities while the rest of the segments have 7 accelerating cavities. The accelerating structure occupies  $7/9^{\text{th}}$  of the real estate in this part of the linac. The first segment uses only 6 cavities to make room for a beam-line vacuum-isolation valve. The field in the first segment is increased to give the same energy gain as the 7 cavity segments. At the end of the normal conducting linac the real estate accelerating field is 1.427 MeV/m at 211 MeV. Figure 4 shows the transverse and longitudinal emittance in the normal conducting linac and the first part of the superconducting linac.

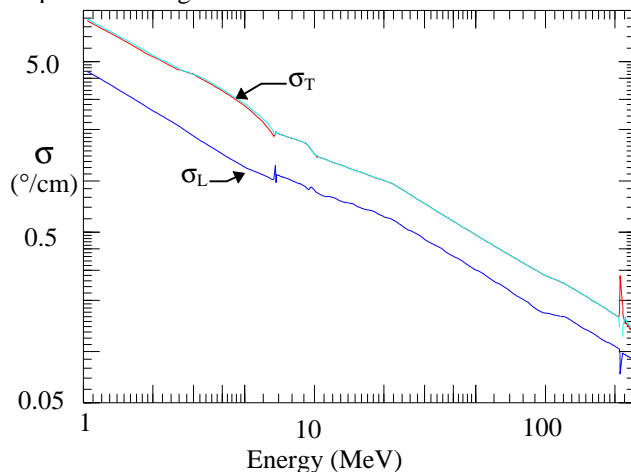


Figure 2. A log-log plot of the longitudinal ( $\sigma_L$ ) and transverse ( $\sigma_T$ ) zero-current phase advance divided by the transverse-focusing-period length. The transition from the quad-singlet focusing in the normal conducting linac to the quad-doublet focusing in the superconducting linac causes the spikes at 211 MeV.

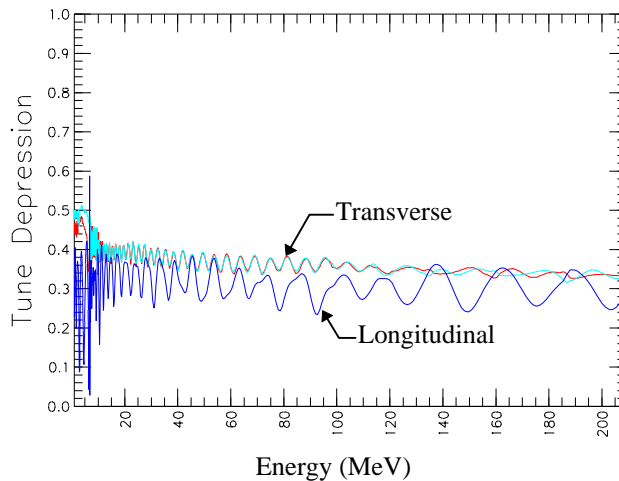


Figure 3. The longitudinal and transverse tune depression from 1.0 MeV to 211 MeV in the APT linac plotted versus energy. The tune depression is the ratio of the phase advance with 100 mA to the phase advance with “zero” current.

### 5 CURRENT INDEPENDENT MATCH

A current independent match means the beam match between two parts of the linac does not depend on the beam current. The APT linac must operate with a 100-mA

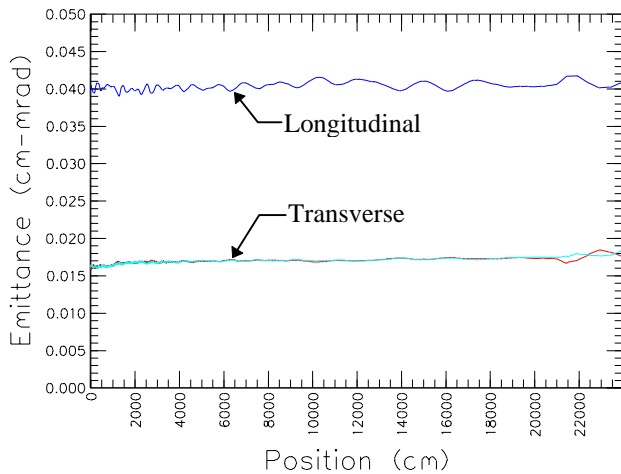


Figure 4. The transverse and longitudinal emittance versus position in the 6.7-MeV-to-211-MeV linac and the first 6 “Cryomodules” of the superconducting linac. The superconducting linac starts at ~21000 cm in this figure.

CW beam. We must keep the beam loss to a very small level even during commissioning. During commissioning we will use beam pulses of about 200  $\mu$ sec duration and with low peak current at first. Under these conditions we can allow a larger fraction of the beam to be lost. Later in the commissioning process the pulsed beam will have a peak current of 100 mA and only a small fraction can be lost. During commissioning with a pulsed beam we will optimize the quadrupole magnet strengths and the RF amplitudes and phases for extremely small beam loss. We must not change these settings for the CW beam. Therefore, we need a current independent match so that we can operate the accelerator at any current up to 100 mA without readjusting the quadrupole focusing magnets or the RF settings. The current independent match between the RFQ and CCDTL has been checked by running PARMTEQ simulations of the RFQ with input beams with currents of 0, 40, 57, 103, and 110 mA. These output beam distributions from the PARMTEQ simulations were then used as the input beam distributions for PARMILA simulations of the beam through the CCDTL and CCL without changing any parameters. The PARMILA code uses the beam current contained in the input distribution file. The match in all cases was satisfactory.

We used the following philosophy throughout the design of the linac to ensure current independent matching between different parts of the linac. We kept the ratio of the longitudinal to the transverse focusing strength nearly constant and without steps in either the longitudinal or transverse focusing strengths. This philosophy results in a linac design with a beam that is nearly equipartitioned [6,7]. With a nearly equipartitioned beam there may be less beam in the halo for a well matched beam such as that shown in Figure 1. Reference [8] shows that a halo can develop even with a well matched beam if it is not

equipartitioned. With a poorly matched beam, a halo will develop whether or not the beam is equipartitioned.

## 6 CONCLUSIONS

The PARMILA design of the normal conducting linac for APT is complete. The simulations show essentially no emittance growth in this linac. The match between the RFQ and the CCDTL is current independent. The match between the various sections of the CCDTL and the CCL is extremely good because there is no change in the transverse focusing period and the variation in the real-estate accelerating field is smooth.

The beam can be matched to the superconducting linac. Although we have not checked this match with a complete set of simulations (only with 0 and 100 mA) we expect the match to the superconducting linac to be current independent, because we kept the focusing strength per cm continuous across this transition.

## REFERENCES

- [1] G. Lawrence, “High Power Proton Linac for APT; Status of Design and Development,” these proceedings.
- [2] H. Takeda, J. H. Billen, “Recent Developments in the Accelerator Design Code PARMILA” these proceedings.
- [3] L. M. Young, “Tuning of the LEDA RFQ 6.7 MeV Accelerator,” these proceedings.
- [4] L. M. Young, “Simulations of the LEDA RFQ 6.7 MeV Accelerator,” Proceedings of the 1997 Particle Accelerator Conference.
- [5] J. H. Billen et al., “A New RF Structure For Intermediate-Velocity Particles” *Proceedings of the 1994 Linear Accelerator Conference*, August 21-26, 1994 Tsukuba, Japan.
- [6] R. A. Jameson, “On Scaling & Optimization of High Intensity, Low-Beam-Loss RF Linacs for Neutron Source Drivers”, AIP Conf. Proc. 279, ISBN 1-56396-191-1, DOE Conf-9206193 (1992) 969-998, Proceedings Third Workshop on Advanced Accelerator Concepts, 14-20 June 1992, Port Jefferson, Long Island, NY, (LA-UR-92-2474, Los Alamos National Laboratory).
- [7] M Reiser, “Theory and Design of Charged Particle Beams,” John Wiley & Sons, Inc., p. 573 (1994).
- [8] L. M. Young, “Equipartitioning in A High current proton Linac”, Proceedings of the 1997 Particle Accelerator Conference.